Int. J. Appl. Ceram. Technol., 13 [3] 480–486 (2016)
DOI:10.1111/ijac.12510

Flexible Nanocomposite Generator Using PZT Nanorods and Ag Nanowires

Woo-Suk Jung†, Min-Jae Lee, and Seok-Jin Yoon

Center for Electronic Materials, Korea Institute of Science and Technology (KIST), Hwarangno 14-gil 5, Seongbuk-gu, Seoul, 136-791, Korea

Won-Hee Lee†

Probe Development Lab, Samsung Medison, Teheran-ro 108-gil, Gangnam-gu, Seoul, 135-851, Korea

Byeong-Kwon Ju

Display and Nanosystem Laboratory, School of Engineering, Korea University, Seoul, 136-713, Korea

Chong-Yun Kang*

Center for Electronic Materials, Korea Institute of Science and Technology (KIST), Hwarangno 14-gil 5, Seongbuk-gu, Seoul, 136-791, Korea

KU-KIST Graduate School of Converging Science and Technology, Korea University, 145, Anam-ro, Seongbuk-gu, Seoul, 136-701, Korea

This study presents a piezoelectric composite generator using PDMS polymer, PZT nanorods, and Ag nanowires. To enhance output power of the generator, we inserted the Ag NWs into the PDMS-PZT composite, which play very important roles in our generator: First, it enables the PZT NRs well distributed in PDMS polymer. Second, it is to reinforce the applied stress of the device by enhancing its flexibility. Finally, conduction paths formed by the Ag networks can reduce the internal resistance of the device. To assess these effects, we have compared and evaluated output voltage and current of four different generators.

Introduction

Nanogenerators based on piezoelectric materials have attracted extensive attentions because they are capable of converting mechanical, vibrational, and hydraulic energy into electricity for powering nanodevices and nanosystems.[1–6] Mechanical energy is the most likely reliable and independent energy source, because it exists everywhere around us such as body movements, vibrations on road and bridge, and people walking and running, regardless of environment such as wind, rain, and temperature.[7–10] After the introduction of piezoelectric ZnO nanowire (NW) in 2006, nanotechnologies such as solar, thermal, and chemical energy harvesting technologies have been made a rapid progress. Recently, increased efforts have been directed toward the ultimate goal of fabricating a flexible, wearable, or implantable energy harvesting systems with realistic power outputs, based on highly efficient piezoelectric nanoassemblies.[11–14] Nevertheless, output power of nanocomposite generators is not enough to use electronics directly as a power source. Herein, we report how to enhance the output power of piezoelectric nanocomposite generator using Ag nanowires (NWs), and introduce a simple, low-cost, and large area fabrication based on $PbZrTiO_3$ nanorods (NRs) synthesized via a hydrothermal reaction. The PZT NRs and Ag NWs are dispersed in polydimethylsiloxane (PDMS) by mechanical agitation to fabricate a piezoelectric nanocomposite. This piezoelectric nanocomposite is spin-casted onto metal-coated plastic substrates and cured in an oven. Under periodic external mechanical deformation by bending stage or mechanical excitation from finger of human body, electric signals are repeatedly generated from the nanocomposite generator.

Experimental Procedure

$PbZrTiO_3$ NRs were synthesized by a hydrothermal method as shown in Fig. 1. The growth solution (50 mL)

†These authors have equal contribution
*cykang@kist.re.kr

was prepared by mixing Ti^{4+} ethanol solution and then added into the Zr^{4+} aqueous solution in the molar ratio of 48:52 (Ti:Zr) under vigorous stirring. The mixed solution was introduced into a 0.15*M* ammonia solution, which resulted in the coprecipitation of $Zr_{0.52}Ti_{0.48}O(OH)_2$ (ZTOH). The ZTOH was filtered several times by DI water, and lead nitrate $Pb(NO_3)_2$, potassium hydroxide (KOH), PVA, and PAA were all added to form the final

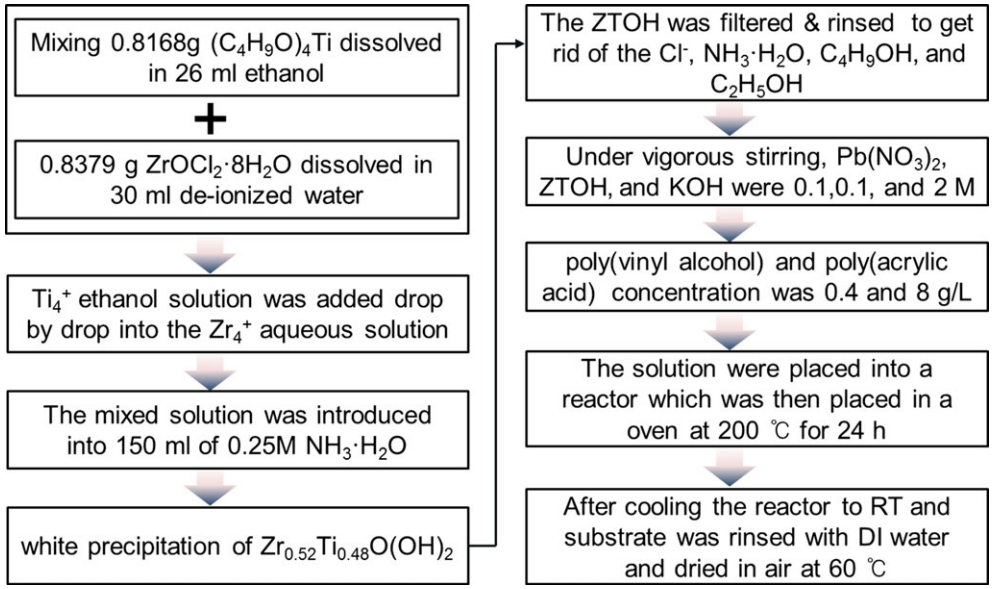

Fig. 1. Hydrothermal process for synthesizing PZT NRs.

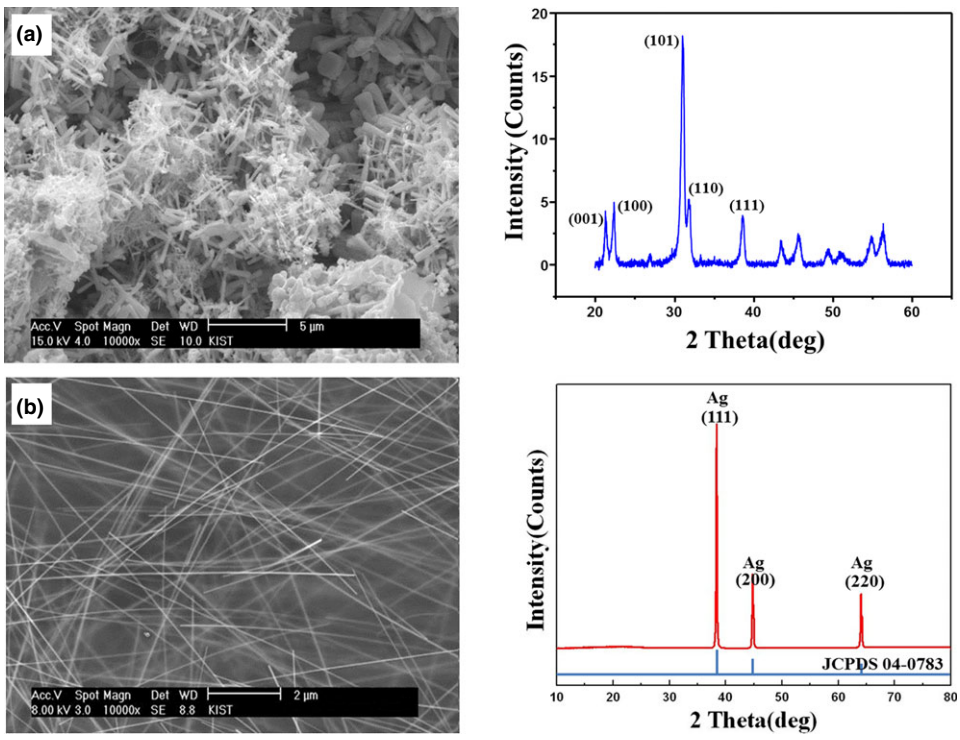

Fig. 2. SEM images of (a) PZT NRs and (b) Ag NWs.

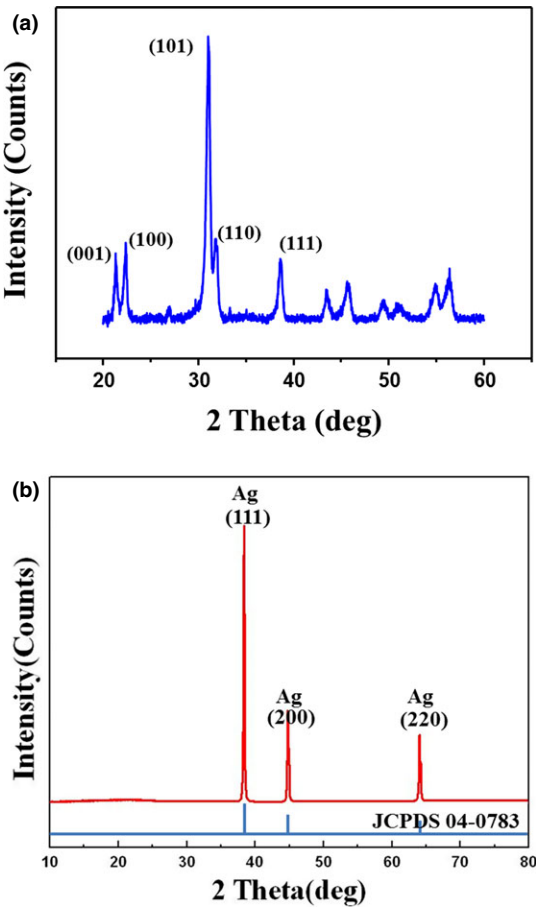

Fig. 3. XRD patterns of (a) PZT NRs and (b) Ag NWs.

hydrothermal solution with a 50 mL total volume. The concentrations of $Pb(NO_3)_2$, ZTOH, and KOH were 0.1, 0.1, and 2*M*, respectively.[15–18] The PVA and PAA concentrations were 0.4 and 8.8 g/L. After stirring for 30 min, this solution was transferred into a 100-mL Teflon-lined stainless steel autoclave to undergo hydrothermal reaction at 200°C. To obtain the NRs, the reaction was performed for 12 h, respectively. The obtained PZT powders were filtered, washed with distilled water, and dried at 70°C for 12 h. As-grown NRs were further annealed at 600°C for 12 h.

The Ag NWs were synthesized by the reduction of Ag nitrate in the presence of polyvinylpyrrolidone (PVP) in ethylene glycol. The Ag NWs were synthesized as follows: 10 mL of ethylene glycol (EG) (99.8%; Sigma-Aldrich, St. Louis, MO) was placed into a round bottom flask, which was heated, using an oil bath, at 160°C. After stabilization, approximately 1 h, 6 mL of a 0.1*M* silver nitrate (99.0%; Sigma-Aldrich) solution in ethylene glycol (EG) and 6 mL of 0.6*M* polyvinylpyrrolidone (PVP), Sigma-Aldrich, in ethylene glycol (EG) were injected drop wise over 5 min into the flask. The mixture was then left reacting for 2 h.[19,20]

Annealed PZT NRs are mixed with Ag NWs. The mixture is then stirred for 5 h in ethanol with a magnetic bar. After the subsequent drying and granulation, the well-mixed nanomaterials (compositions of 1 wt% Ag NWs and 12 wt% $PbZrTiO_3$ NRs) are poured into a PDMS matrix for the final nanocomposite. The nanocomposite is spin coated on the Au/Cr-coated kapton polyimide film at 1000 rpm for 15 s and cured at

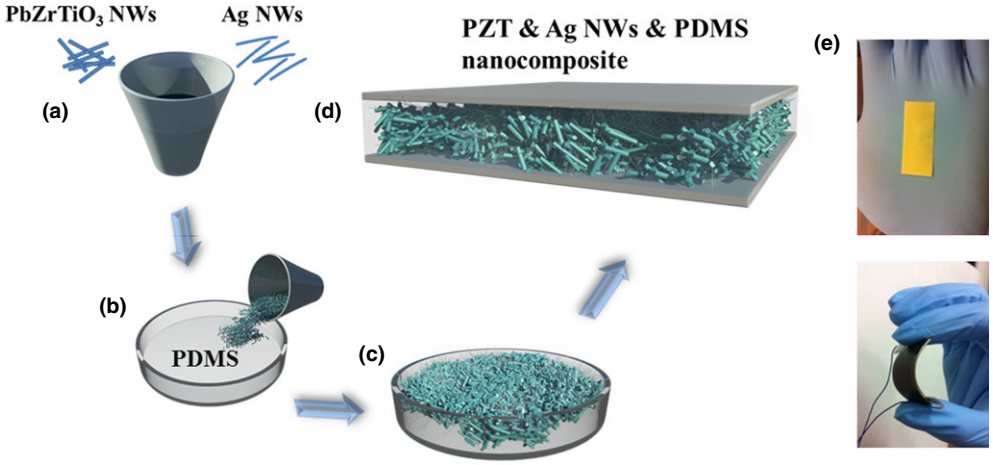

Fig. 4. Schematic illustration of the process for fabricating NCG. (a) The PZT and Ag nanostructures are poured into a petri dish and (b) cured at room temperature for a day. (c) The "piezoelectric rubber" bulk-type NCG isolated with Ag paste which are used to top/bottom electrodes. (d) PDMS-PZT-Ag NCG (e) Feature of the fabricated flexible NCG.

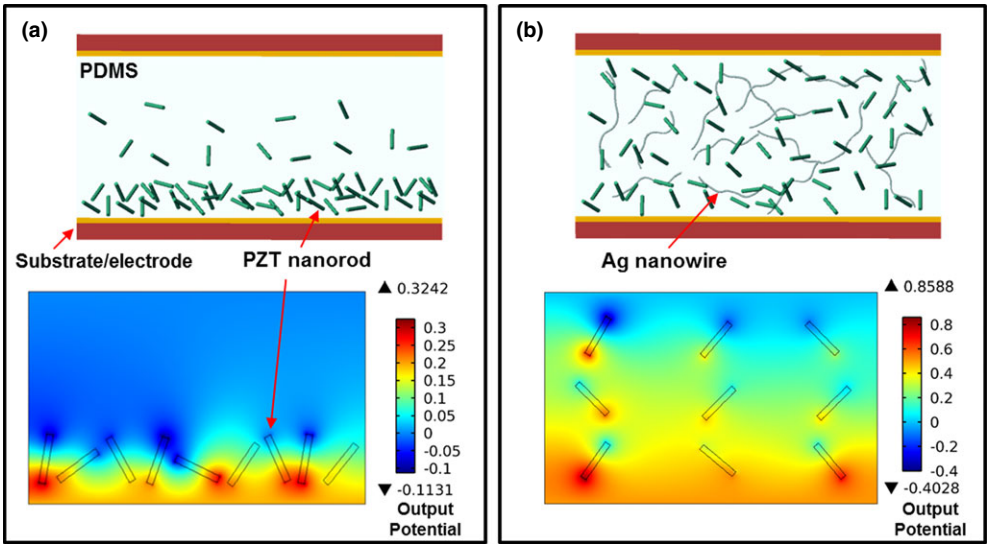

Fig. 5. Cross-sectional view and output potential of (a) the PDMS-PZT NCG and (b) PDMS-PZT-Ag NCG.

80°C for 10 min in an oven. The 100-nm-thick Au and 30-nm-thick Cr were deposited on Kapton film by DC sputter. Another Au/Cr-coated Kapton film was attached to the surface of the spin-coated nanocomposite. The Kapton film sandwiched nanocomposite was finally attached to polyester (PS) film. We applied ~100 kV/cm of electric field for electric poling electric poling at room temperature.[21] The wires are attached to metal pads by means of silver (Ag) paste for the characterization of the output voltage and current signals. A linear motor was used to periodically apply and release the compressive force.

Results and Discussion

Figures 2a and b show scanning electron microscopy (SEM) images of the PZT NRs and Ag NWs. The morphology of the PZT NRs was prepared by the hydrothermal reaction method assisted using PVA/PAA. Without polymer surfactants, PZT particles prepared by the hydrothermal method using a high concentration of KOH as the mineralizer are cubic in shape. The PZT NRs (about 200 nm in diameter and about 3–7 μm in length) are obtained when polymer surfactants were introduced in the hydrothermal reaction system. Figure 2b shows a uniform and well ordered of the Ag NWs where the length varied approximately 10–20 μm with a diameter of 50–100 nm.

Figure 3a presents the X-ray diffraction (XRD) patterns of the PZT NRs under hydrothermal condition. A simple identification indicates that the powders have a tetragonal PZT structure, which agree well with the literature values of $a = 4.036$ and $c = 4.146$ (JCPDS, file no. 33-0784). It can be concluded from Figure 3a that the powders are well crystallized. The XRD spectrum of the Ag nanowire arrays is shown in Figure 3b. It can be seen that there are three peaks in the XRD spectra of the Ag nanowire arrays. They are, respectively, corresponding to the (111), (200), and (220) planes. All the intense XRD peaks can be indexed to the face-centered-cubic phase of silver according to the literature pattern (JCPDS no. 04-0783).

Figure 4 shows the fabricated flexible nanocomposite generator and its fabrication procedure. The piezoelectric nanogenerator mainly consists of three layers, two Kapton films with Au/Cr electrodes and the PZT-Ag nanostructures mixed with the PDMS composite which serves as a source of piezoelectric potential. Due to the use of all polymer layers in our nanogenerator, the device could be easily bent and released for the generation of electricity. As shown in Figure 2a, the growth direction of the PZT NR is not parallel to any crystallographic axes. Therefore, the electric dipoles are neither parallel nor perpendicular to the growth direction of the nanowire. Furthermore, the NWs are randomly oriented inside the PDMS polymer.

When the high electric field is applied, the electric dipoles would tend to align along the electric field direction. Some ferroelectric domains will align along the electric field direction, while some domains may tilt from the electric field direction. However, all of the domains have electric dipole components along the electric field direction. For each PZT NR, we simply consid-

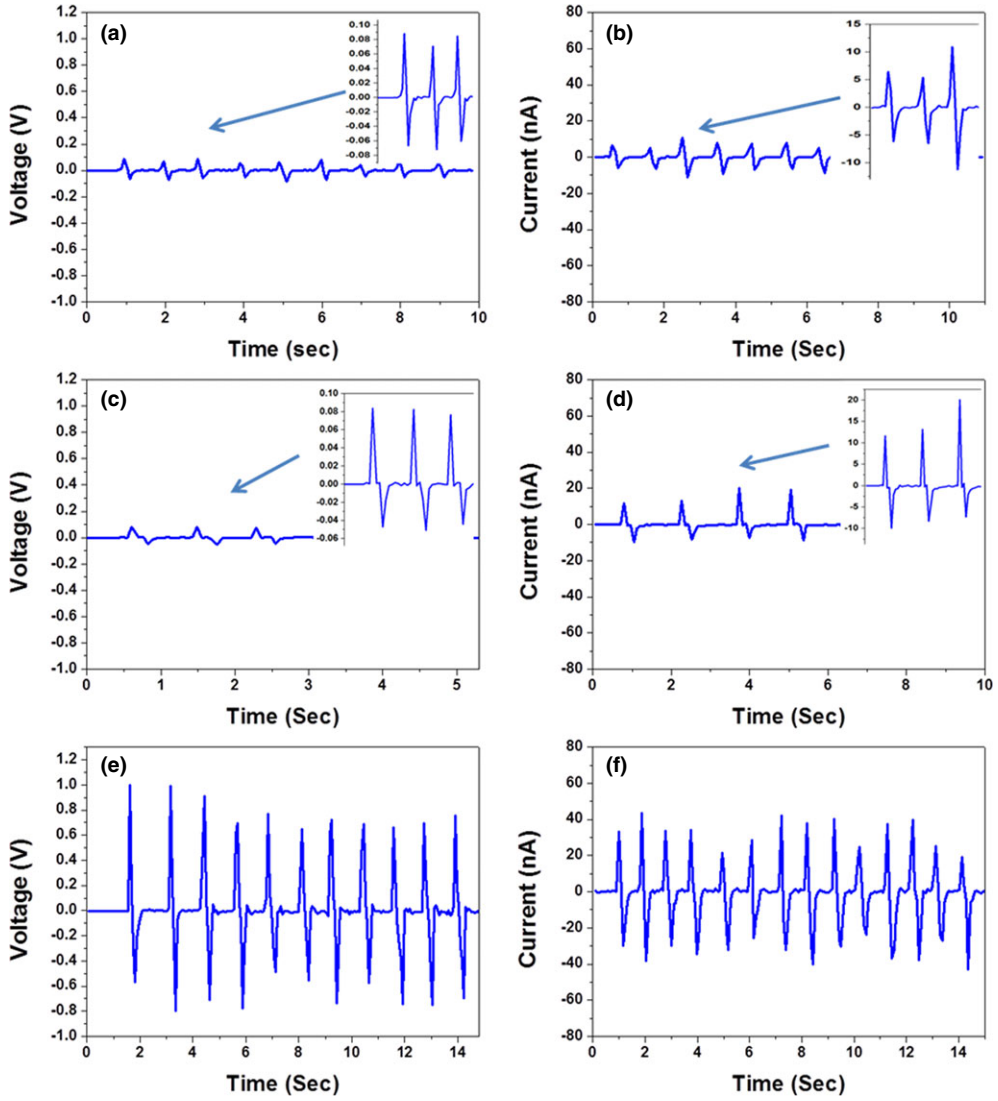

Fig. 6. Output voltage and current of (a) and (b) PDMS device, (c) and (d) PDMS-Ag device, and (e) and (f) PDMS-PZT device.

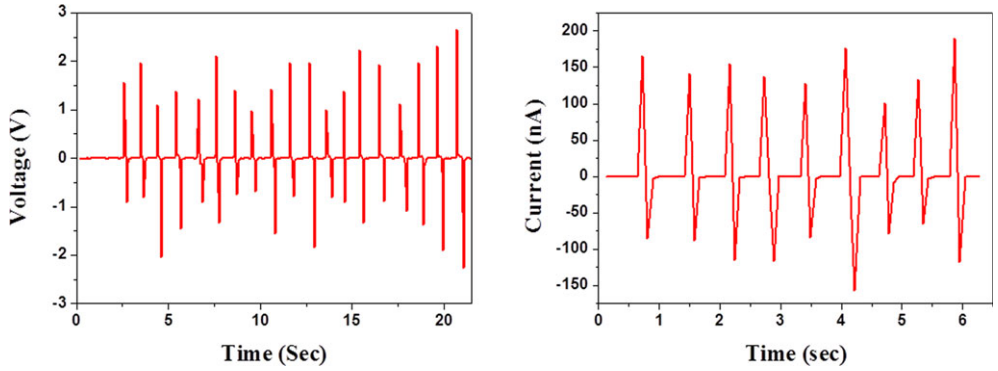

Fig. 7. Output voltage and current of PDMS-PZT-Ag NCG.

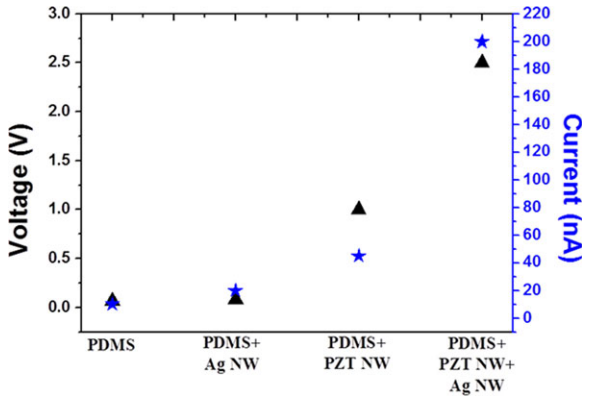

Fig. 8. Comparison on output voltage and current of four different devices.

ered the same electric dipole component along the electric field direction. In the case of the PZT nanocomposite with Ag NWs, we expect the PZT NRs can be well distributed by forming a complex mixture with the Ag NW networks, which the nanowires act as a dispersing agent, as shown in Figure 5. Therefore, the dispersed one by Ag nanowires produces a higher output potential than the other one because the Ag NW is to reinforce the stress applied to the generator by enhancing the composite stress. It makes the generator more flexible due to the change of the mechanical properties of the composite material.[22] The Ag NWs are mixed and entangled with PZT NRs in PDMS matrix, and the distributed PZT NWs can significantly be stressed. Finally, the conduction paths formed by the Ag networks in PDMS matrix effectively reduce the internal resistance of nanocomposite generator, which results in increase of the piezoelectric output potential.[23] The photograph in Figure 4e shows the final generator. To clearly understand, the enhanced output power of flexible nanocomposite generator using PZT NRs and Ag NWs, we performed experiment with four different devices: (1) The power generation only from the PDMS polymer without PZT NRs and Ag NWs. (2) PDMS-Ag nanocomposite device. (3) PDMS-PZT nanocomposite device (4) PDMS-PZT-Ag nanocomposite device. We confirmed the power generation from the all samples fabricated using the same dimension and mixing ration with PDMS. We measured the NC generator during periodic bending and unbending motion of the bending. We obtained the output voltage and current from the PDMS and PDMS-Ag devices are much lower than PDMS-PZT device as shown in Figure 6. Furthermore, peak output voltage and peak output current of PDMS-PZT-Ag device reached ~1.7 V and ~130 nA, respectively, as shown in Figure 7. Figure 8 shows a comparison on output voltage and current of all different devices. From this experiment, it shows that Ag NWs is effective way to enhance output power of the nanocomposite generator. We also tested the stability of the PZT nanocomposite generator by continuously applying and releasing the compressive strain. During almost 1600 s, while there are some fluctuations, the output voltage and current are stable as shown in Figure 9.

Conclusions

We have fabricated the nanocomposite generator based on the piezoelectric PZT NRs and Ag NWs, in which Ag NWs play a role in enhancing output power. To confirm this effect, we have compared output voltage

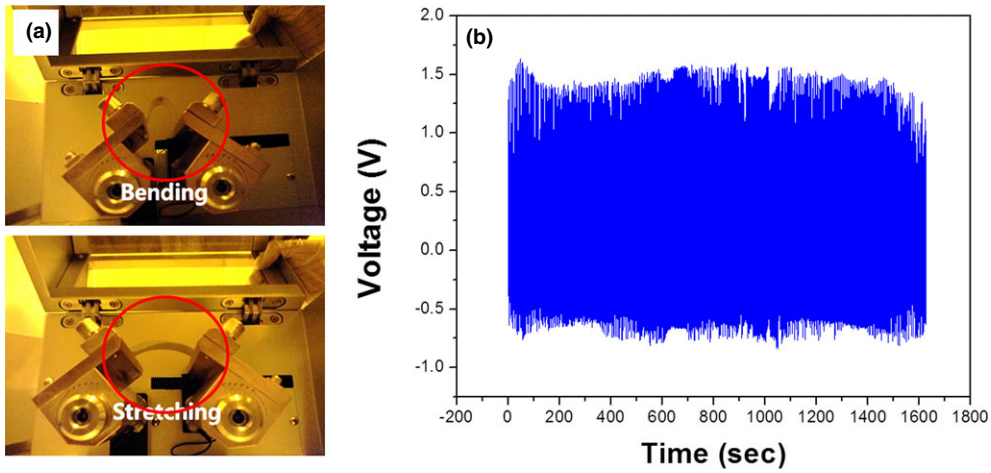

Fig. 9. Stability test of PDMS-PZT-Ag NCG.

and current of four different generators: PDMS, PDMS-Ag, PDMS-PZT, and PDMS-PZT-Ag devices. From the experimental results, PDMS-PZT-Ag nanocomposite generator is superior to output power, in which Ag NWs increases both output voltage and output current of the device. We obtained that the maximum output voltage and current of the generator were ~2.5 V and ~ 200 nA, respectively. Our piezoelectric nanocomposite technique successfully overcomes the size-related restrictions existed in previous nanogenerator and enables simple, low-cost, and large-scale self-powered energy system. We expect that the piezoelectric nanocomposite generator is a valuable candidate for a consumer electronics, sensor networks and energy harvesting devices.

Acknowledgment

This work was supported by the Energy Technology Development Project (KETEP) grant funded by the Ministry of Trade, Industry and Energy, Republic of Korea (Piezoelectric Energy Harvester Development and Demonstration for scavenging Energy from Road Traffic System, project No. 20142020103970), the Institutional Research Program of the Korea Institute of Science and Technology (2E25440), and KU-KIST Research Program of Korea University (R1309521).

References

1. A. Testino, *Int. J. Appl. Ceram. Technol.*, 10 [5] 723–730 (2013).
2. J. P. Holdren, *Science*, 315 721–896 (2007).
3. S. H. Lee, W. B. Ko, and J. Hong, *J. Nanosci. Nanotechnol.*, 14 [12] 9319–9322 (2014).
4. G. Zhu, A. C. Wang, Y. Liu, Y. Zhou, and Z. L. Wang, *Nano Lett.*, 12 3086–3090 (2012).
5. K. I. Park, *et al.*, *Nano Lett.*, 10 4939–4943 (2010).
6. J. H. Jung, *et al.*, *ACS Nano*, 5 10041–10046 (2011).
7. S. Xu, Y. Qin, C. Xu, Y. Wei, R. Yang, and Z. L. Wang, *Nat. Nanotechnol.*, 5 366–373 (2010).
8. M. B. Lee, *et al.*, *Adv. Mater.*, 24 1759 (2012).
9. Z. L. Wang, *Sci. Am.*, 298 82–87 (2008).
10. Z. L. Wang, *Adv. Funct. Mater.*, 18 3553 (2008).
11. Z. L. Wang and J. Song, *Science*, 312 242–246 (2006).
12. S. Xu, B. Hansen, and Z. L. Wang, *Nat. Commun.*, 1 93 (2010).
13. X. Wang, *Nano Energy*, 1 [1] 13–24 (2012).
14. K. I. Park, S. B. Bae, S. H. Yang, H. I. Lee, K. Lee, and S. J. Lee, *Nanoscale*, 6 8962 (2014).
15. G. Xu, Z. Ren, P. Du, W. Weng, G. Shen, and G. Han, *Adv. Mater.*, 17 907–910 (2005).
16. Z. Ren, G. Xu, X. Wei, Y. Liu, G. Shen, and G. Han, *J. Am. Ceram. Soc.*, 90 2645 (2007).
17. X. Yang, Y. Zhao, Y. Yang, and Z. Dong, *Mater. Lett.*, 61 3462 (2007).
18. P. Y. Deng, *et al.*, *Mater. Lett.*, 63 937 (2009).
19. L. Gou, M. Chipara, and J. M. Zaleski, *Chem. Mater.*, 19 1755–1760 (2007).
20. J. Y. Lee, S. T. Connor, Y. Cui, and P. Peumans, *Nano Lett.*, 8 [2] 689–692 (2008).
21. Y. Ting, H. Gunawan, J. Z. Zhong, and C. W. Chiu, *J. Eur. Ceram. Soc.*, 34 [11] 2849–2855 (2014).
22. I. Seshadri, G. Esquenazi, T. Borca-Tasciuc, P. Keblinski, and G. Ramanath, *Appl. Phys. Lett.*, 105 01310 (2014).
23. C. Seoul, Y. T. Kim, and C. K. Baek, *J. Polym. Sci., Part B: Polym. Phys.*, 41 [13] 1572–1577 (2003).